

THE FORMATION OF SUPERMASSIVE BLACK HOLES FROM POPULATION III SEEDS. I. COSMIC FORMATION HISTORIES

NILANJAN BANIK¹

Dept. of Physics, University of Florida, Gainesville, FL 32611, USA,
Fermi National Accelerator Laboratory, Batavia, IL 60510-0500, USA.

JONATHAN C. TAN²

Depts. of Astronomy and Physics, University of Florida, Gainesville, FL 32611, USA

PIERLUIGI MONACO³

Università di Trieste, Dipartimento di Fisica, Sezione di Astronomia, via Tiepolo 11, 34143 Trieste – Italy,
INAF–Osservatorio Astronomico di Trieste, via Tiepolo 11, 34143 Trieste – Italy,
INFN, via Valerio 2, I-34127 Trieste, Italy

ABSTRACT

We model the cosmic distributions in space and time of the formation sites of the first stars that may be progenitors of supermassive black holes (SMBHs). Such Pop III.1 stars are defined to form in dark matter minihalos with $\sim 10^6 M_{\odot}$ that are isolated from neighboring astrophysical sources by a given isolation distance, d_{iso} . We assume Pop III.1 sources are seeds for the cosmic population of SMBHs, based on a model of protostellar support by dark matter annihilation heating that allows them to accrete most of the baryonic content of their minihalos, i.e., $\gtrsim 10^5 M_{\odot}$. Exploring a range of d_{iso} from 10 to 100 kpc (proper distances), we predict the redshift evolution of the number density of Pop III.1 sources and their SMBH remnants. The local, $z = 0$ density of SMBHs constrains $d_{\text{iso}} \gtrsim 100$ kpc (i.e., 3 Mpc comoving distance at $z \simeq 30$). In our simulated $(40.96 h^{-1} \text{Mpc})^3$ comoving volume, Pop III.1 stars start forming just after $z = 40$. Their formation is largely complete by $z \simeq 25$ to 20 for $d_{\text{iso}} = 100$ to 50 kpc. We follow source evolution down to $z = 10$, by which point SMBHs reside in halos with $\gtrsim 10^8 M_{\odot}$. Over this period, there is relatively limited merging of SMBHs for these values of d_{iso} . We also predict clustering properties of SMBHs at $z = 10$: the effective feedback suppression of neighboring sources in the $d_{\text{iso}} = 100$ kpc model leads to a relatively flat angular correlation function. The general results of this work will be used for population synthesis models of active galactic nuclei to be compared with future high redshift observations.

1. INTRODUCTION

Baryonic collapse appears to lead to two distinct populations of objects: (1) stars (and associated planets); (2) supermassive black holes (SMBHs). SMBHs have masses $\gtrsim 10^5 M_{\odot}$ and are found in the centers of most large galaxies (e.g., Kormendy & Ho 2013; den Brok et al. 2015; see review by Graham 2016). Some SMBHs appear to have reached masses $\sim 10^9 M_{\odot}$ by $z \simeq 7$ ($t \simeq 800$ Myr after the Big Bang) (e.g., Mortlock et al. 2011; however, see the factor of ~ 5 lower revised mass estimates of Graham et al. 2011; Shankar et al. 2016).

SMBH formation scenarios include “direct collapse of massive gas clouds,” which are thought to require strong UV radiation fields to dissociate H_2 molecules and thus prevent cooling to ~ 200 K and fragmentation to $\sim 100 M_{\odot}$ mass scales (e.g., Haehnelt & Rees 1993; Bromm & Loeb 2003; Begelman et al. 2006; Dijkstra et al. 2006; Ferrara & Loeb 2013; Dijkstra et al. 2014), rapid infall of gas driven by galaxy mergers (Mayer et al. 2010; 2015) or else strong shocks in or between proto-galaxies (Inayoshi & Omukai 2012; Inayoshi et al. 2015). These models generally involve complex

accretion flows and/or feedback environments that make model predictions very uncertain, e.g., for how often SMBH formation occurs.

Another scenario involves a very massive stellar seed forming in the center of a dense stellar cluster by a process of runaway mergers (Gürkan et al. 2004; Portegies Zwart et al. 2004; Freitag et al. 2006). However, the required stellar densities are extremely high (never yet observed in any cluster) and also stellar wind mass loss may make growth of the central very massive star quite inefficient (Vink 2008), unless the metallicities are very low (Devecchi et al. 2012). Again, predictions of such models for the cosmic formation rates of SMBHs are limited since it is difficult to predict when and how the necessary very dense star clusters are formed.

Yet another scenario proposes that SMBHs form from the remnants of Population III (Pop III) stars, i.e., those forming from metal-free gas with compositions set by big bang nucleosynthesis (BBN). McKee & Tan (2008) distinguished two classes of Pop III stars. Pop III.1 are those that form in isolation from any significant influence of any other astrophysical source (i.e., other stars or SMBHs). Molecular Hydrogen cooling leads to ~ 200 K temperatures in the centers of minihalos and first unstable fragment scales of $\sim 100 M_\odot$ (Bromm et al. 2002; Abel et al. 2002). Pop III.2 stars are influenced by such sources, with the most important effect expected to be radiation feedback from ionizing or dissociating radiation (e.g., Whalen et al. 2008). The masses of Pop III.2 stars are thought to be significantly smaller than those of Pop III.1 stars due to enhanced electron fractions in the irradiated gas that promotes H_2 and HD formation (Greif & Bromm 2006).

However, the ultimate masses of Pop III.1 stars are quite uncertain. McKee & Tan (2008) presented semi-analytic estimates for masses of $\sim 140 M_\odot$ set by disk photoevaporation feedback. Hosokawa et al. (2011) found similar results using radiation-hydro simulations. Tan, Smith & O’Shea (2010) applied the MT08 model to accretion conditions in 12 minihalos from the simulations of O’Shea et al. (2007) and estimated an initial mass function that peaked at $\sim 100 M_\odot$ with a tail extending to $\sim 10^3 M_\odot$. Hirano et al. (2014) and Susa et al. (2014) presented radiation-hydro simulations of populations of ~ 100 Pop III.1 stars, deriving initial mass functions peaking from ~ 10 – $100 M_\odot$, with a tail out to $\sim 10^3 M_\odot$. Their formation redshifts extended from $z \sim 35$ down to $z \sim 10$.

While the above estimates for Pop III.1 masses are certainly top heavy compared to present-day star formation, they are still relatively low compared to the masses of SMBHs. To reach $\sim 10^9 M_\odot$ in a few hundred Myr would require near continuous maximal (Eddington-limited) accretion. Such accretion seems unlikely given that massive Pop III.1 stars would disrupt the gas in their natal environments by radiative and mechanical feedback (e.g., O’Shea et al. 2005; Johnson & Bromm 2007; Milosavljević et al. 2009).

One potential mechanism that may allow supermassive Pop III.1 stars to form is heating by Weakly Interacting Massive Particle (WIMP) dark matter self-annihilation (Spolyar et al. 2008; 2009; Natarajan, Tan & O’Shea 2009, hereafter NTO09), which may keep the protostar large and cool, so limiting its ionization feedback. NTO09 estimated that for the early phases of protostellar evolution to be significantly affected by WIMP annihilation heating the WIMP mass needs to be $m_\chi \lesssim$ several $\times 100$ GeV. Such WIMP masses are consistent with recent estimated constraints on m_χ based on constraints on the WIMP annihilation cross section coupled with the requirement that the actual cross section should equal the thermal relic value of $\sim 3 \times 10^{-26} \text{ cm}^3 \text{ s}^{-1}$ (i.e., that necessary for all, or most, dark matter to be composed of WIMPs). For example, from particle production in colliders, Khachatryan et al. (2016) find $m_\chi \gtrsim 6$ to 30 GeV depending on whether the process is mediated via vector or axial-vector couplings of Dirac fermion dark matter. From indirect searches via Fermi-LAT observations of expected gamma ray emission from 15 Milky Way dwarf spheroidal satellite galaxies with modeled dark matter density structures, Ackermann et al. (2015) report $m_\chi \gtrsim 100$ GeV for WIMPs annihilating via quark and τ -lepton channels. Such results suggest there is only a relatively narrow range of WIMP masses that are viable for this scenario of dark matter powered Pop III.1 protostars.

Also, direct detection experiments that constrain (spin dependent and independent) WIMP-nucleon elastic scattering cross sections have yet to detect signatures of WIMP dark matter (e.g., Agnese et al. 2014; Akerib et al. 2016). While these results do not provide a firm constraint on the value of m_χ , they do have implications for the ability Pop III.1 protostars to capture WIMPs of a given mass via such scattering interactions.

Spolyar et al. (2009) followed the growth of Pop III.1 protostars including the effects of annihilation heating from their initial and captured dark matter. We note that such dark matter powered protostars are objects that collapse to densities quite similar to those of normal protostars: e.g., for the initial model considered by Spolyar et al., which has $3 M_\odot$ and soon achieves a radius of $\sim 3 \times 10^{13} \text{ cm}$, i.e., $\sim 2 \text{ AU}$, the central densities are $n_{H,c} \sim 6 \times 10^{17} \text{ cm}^{-3}$ and the mean densities $\bar{n}_H \sim 3 \times 10^{16} \text{ cm}^{-3}$. In their canonical case without captured WIMPs collapse of the protostar to main sequence was delayed until about $800 M_\odot$. They also considered a “minimal capture” case with background dark matter density of $\rho_\chi = 1.42 \times 10^{10} \text{ GeV cm}^{-3}$ and $\sigma_{sc} = 10^{-39} \text{ cm}^2$ (for spin-dependent scattering relevant to H) that results in about half the luminosity being from annihilation of captured WIMPs (with $m_\chi = 100 \text{ GeV}$) and the other

half from nuclear fusion at the time the protostar joins the main sequence. The results from Akerib et al. (2016) imply this $\sigma_{\text{sc}} \lesssim 5 \times 10^{-39} \text{ cm}^2$, so the fiducial capture model of Spolyar et al. is still allowed by recent dark matter search constraints. While Spolyar et al. (2009) presented a case in which the protostar reached $\sim 1000 M_{\odot}$, depending on the WIMP mass and the capture history of dark matter to the protostar, much larger masses, $\gtrsim 10^4 M_{\odot}$ are possible (Chanchaiworawit & Tan, in prep.).

However, WIMP annihilation heating is only expected to be significant in Pop III.1 protostars if these objects are co-located near the peaks of their natal dark matter minihalos. Such co-location may be disturbed if Pop III.1 star formation involves substantial fragmentation, e.g., leading to binary star or multiple star formation, that results in the primary star being displaced from the “central region” of the dark matter cusp. As discussed above, Spolyar et al. (2009) have presented a case in which effective WIMP annihilation heating alters the evolution of the protostar for a dark matter density of $\rho_{\chi} \gtrsim 10^{10} \text{ GeV cm}^{-3}$. For the three example minihalos considered by NTO09, the initial radii defining such a central region are 72, 45 and 89 AU. In the simulation of Stacy et al. (2014), which follows the interaction of an “active” dark matter halo that has its central density reduced by interactions with a clumpy accretion disk, this radius is still $\sim 40 \text{ AU}$ at the end of their simulation, 5000 yr after first protostar formation.

Limited fragmentation during initial collapse of minihalos was seen in the cosmological simulations of Turk, Abel & O’Shea (2009): about 80% of their minihalos appear to collapse to a single protostellar “core,” i.e., the self-gravitating gas in which a single rotationally supported disk will form. However, a number of authors have claimed that later fragmentation of the primary protostar’s accretion disk may lead to formation of multiple lower mass stars leading to either formation of a close binary or even a cluster of Pop III stars. Clark et al. (2011) followed the evolution to about 110 yr after first protostar formation, including effects of protostellar heating on the disk. By this time the protostar had accreted almost $0.6 M_{\odot}$. It still resided near the center of its accretion disk, which, being gravitationally unstable, had also formed three lower mass ($\lesssim 0.15 M_{\odot}$) protostars. Greif et al. (2011) followed the collapse and fragmentation of five different minihalos to about 1000 yr after first protostar formation, by which time masses of several solar masses had been achieved. They typically observed several tens of protostars forming by fragmentation in the main accretion disk, although describe that most are likely susceptible to merging with the primary protostar (a process they could not follow in their simulations).

Smith et al. (2012) carried out similar simulations, but now including the effects of WIMP annihilation on the chemistry and thermodynamics of the collapse. They found much reduced fragmentation: in one case only a single, primary protostar formed; in another, just one secondary protostar. The primary protostars reached $\gtrsim 10 M_{\odot}$ and remained in the central regions of their host minihalos. Stacy et al. (2014) also carried out such simulations, but now with no protostellar heating feedback. They formed a primary protostar that reached $8 M_{\odot}$ after 5000 yr along with several lower-mass companions. This primary protostar was still located in a zone with dark matter density $\rho_{\chi} \gtrsim 10^{10} \text{ GeV cm}^{-3}$.

However, the propensity of protostellar accretion disks to fragment will also depend on the magnetic field strength in the disk and none of the above fragmentation studies have included B -fields. Dynamo amplification of weak seed fields that arise via the Biermann battery mechanism may occur in turbulent protostellar disks: see, e.g., Tan & Blackman (2004); Schleicher et al. (2010); Schober et al. (2012); Latif & Schleicher (2016). These studies all predict that dynamically important, near equipartition B -fields will arise in Pop III protostellar disks. From numerical simulations of local star formation it is well known that such B -fields generally act to suppress fragmentation compared to the unmagnetized case (e.g., Price & Bate 2007; Hennebelle et al. 2011). Magnetic fields would similarly be expected to reduce the density fluctuations in the accretion disks and the size of the disks, which would then reduce the amount of gravitational interaction that is seen to dilute the dark matter density cusp in the simulation of Stacy et al. (2014). If early fragmentation is suppressed then this may allow the primary protostar to achieve a significant mass and luminosity that its radiative feedback then later becomes the dominant means of limiting fragmentation.

In summary, whether or not a single dominant, centrally-located protostar is the typical outcome of collapse of minihalos is still uncertain. Such outcomes are seen in some pure hydrodynamic simulations of collapse, especially when the effects of dark matter annihilation heating are included. If magnetic fields can be amplified to near equipartition by an accretion disk dynamo, then this outcome is expected to be even more likely to occur.

On the other hand, Pop III.2 stars, if formed in a minihalo that undergoes very significant early stage fragmentation to multiple “cores,” are not generally expected to be co-located with the dark matter density peak. Co-location will also not occur for stars forming in more massive halos, where gas atomic cooling allows formation of a large scale rotational supported thin disk, which then fragments to form the stellar population, i.e., the early stages of a galactic disk.

We thus regard formation of dark matter powered Pop III.1 stars as a potentially attractive mechanism to explain the

origin of, potentially all, supermassive black holes. If most of the initial baryonic content of the Pop III.1 minihalos, i.e., $\gtrsim 10^5 M_\odot$, is able to be accreted to the protostar, which then undergoes the general relativistic instability leading to direct collapse to a black hole, then this would explain the absence of supermassive black holes with masses $\lesssim 10^5 M_\odot$. This lower limit to the masses of SMBHs is not easily explained in other formation models.

Our goal in this paper is to assess the predictions of such a model for the formation of SMBHs via the statistics of minihalos that are likely to undergo Pop III.1 star formation, especially their formation history, their overall number density and their clustering properties. The radiative influence on a halo from a neighboring source and its effect on subsequent star formation is a very complicated problem (e.g., Whalen et al. 2006). For simplicity we will therefore parameterize the required “isolation distance,” d_{iso} , that is needed for a given halo to be considered “undisturbed” from other astrophysical sources and thus be able to form a supermassive Pop III.1 star that becomes a SMBH. Future papers will then consider more detailed, physical models for this isolation distance.

2. METHODS

We utilize PINOCCHIO (PINpointing Orbit Crossing Collapsed Hierarchical Objects), which is a code based on Lagrangian Perturbation Theory (LPT) (Moutarde et al. 1991; Buchert & Ehlers 1993; Catelan 1995) for the fast generation of catalogs of dark matter halos in cosmological volumes. Starting from a realization of a Gaussian density field in a box sampled by N^3 particles, using an ellipsoidal collapse model, the code computes the time at which each particle is expected to suffer gravitational collapse (i.e., “orbit crossing,” when the map from initial, Lagrangian, to final, Eulerian positions becomes multivalued), then collects the collapsed particles into halos with an algorithm that mimics their hierarchical clustering. The result is a catalog of dark matter halos with known mass, position, velocity and merger history.

The code was introduced in its original form by Monaco, Theuns & Taffoni (2002), where it was demonstrated that it can accurately reproduce “Lagrangian” quantities like halo masses and merger histories. This was later confirmed by other groups (see the review in Monaco et al. 2013). A massively parallel version was presented by Monaco et al. (2013) and recently extended and tested by Munari et al. (2016). In this last paper it was shown how the clustering of halos improves when higher orders of LPT are used. As a result, clustering in k -space is well reproduced, to within a few per cent, up to a wavenumber of at least $k = 0.3 h \text{ Mpc}^{-1} = 0.203 h_{0.68} \text{ Mpc}^{-1}$, where $h_{0.68} \equiv h/0.6774 = 1$ is the normalized Hubble parameter and will be used in lieu of h henceforth. A degradation of quality is seen at $z < 0.5$, where the density field becomes significantly non-linear. Clustering in configuration space is very well reproduced on comoving scales larger than $(10 - 20)h^{-1} \text{ Mpc} = (14.76 - 29.52)h_{0.68}^{-1} \text{ Mpc}$.

In this paper we use the latest code version with 2LPT displacements, that give a very good reproduction of clustering while keeping memory requirements to ~ 150 bytes per particle, thus allowing running of large boxes (3LPT would require nearly twice as much memory). PINOCCHIO is well-suited to the study of the formation of first stars and SMBHs from high z , relatively low-mass halos spanning large cosmological volumes.

Adopting a standard Planck cosmology: $\Omega_m = 0.3089$, $\Omega_\Lambda = 0.6911$, $n_s = 0.9667$, $\sigma_8 = 0.8159$, $\Omega_b h^2 = 0.02230 = \Omega_b h_{0.68}^2 = 0.0102$, $w_0 = -1$, $w_1 = 0$ (Planck collaboration 2015), we simulate a $40.96 h^{-1} = 60.47 h_{0.68}^{-1} \text{ Mpc}$ comoving cubical box sampled with 4096^3 particles, thus reaching a particle mass of $1.2 \times 10^5 M_\odot$. This allows us to sample a $10^6 M_\odot$ halo with ~ 10 particles. We first run the simulation down to redshift of 15. This required 10 Pb of RAM and took less than an hour on 1376 cores of the GALILEO@CINECA machine, most of the time being spent in writing 211 outputs from $z = 36$ to $z = 15$ in redshift steps of $\Delta z = 0.1$. We then continued the simulation down to $z = 10$, outputting in steps of $\Delta z = 1$. This is the largest PINOCCHIO run ever presented in a paper.

From the simulation outputs, we identify halos that form Pop III.1 stars by looking for minihalos with masses just crossing a threshold of $10^6 M_\odot$, which are also isolated from any other minihalos (i.e., that host Pop III.1, Pop III.2 or Pop II sources) by a proper distance of d_{iso} . We consider values of $d_{\text{iso}} = 10, 20, 30, 50, 100, 300 \text{ kpc}$.

Once halos have been tagged as being Pop III.1 sources we then track their subsequent evolution. For the next 10 Myr after the start of their formation they are assumed to be Pop III.1 stars. This would correspond to the accretion timescale to build up a $10^5 M_\odot$ star if its accretion rate were $10^{-2} M_\odot \text{ yr}^{-1}$, a typical accretion rate expected for such sources (e.g., Tan & McKee 2004). After 10 Myr, the Pop III.1 star is assumed to collapse into a SMBH remnant. The halo containing this remnant is tracked down to $z = 10$. The halo grows in mass by both accretion of dark matter particles (i.e., sub-minihalos) and by merger with already identified minihalos and larger halos. During a merger of two halos, the more massive halo retains its identity and typically the SMBH will be occupying the more massive of the two merging halos. Occasionally the SMBH and its host halo merge with a more massive halo, in which case the presence of the SMBH is transferred to this new halo. Sometimes two merging halos will each already host a SMBH: this situation is expected to lead to SMBH-SMBH binary in the center of the new halo and thus potentially a

merger of the two black holes.

In this paper we focus on SMBH locations, number densities and host halo properties, and defer modeling of SMBH growth due to gas accretion (i.e., active galactic nuclei) to a future paper. While we note when SMBH mergers are expected to occur, we also defer analysis of these merger properties to a future study.

3. RESULTS

3.1. Cosmic Evolution of the Number Density of Pop III.1 Stars and SMBHs

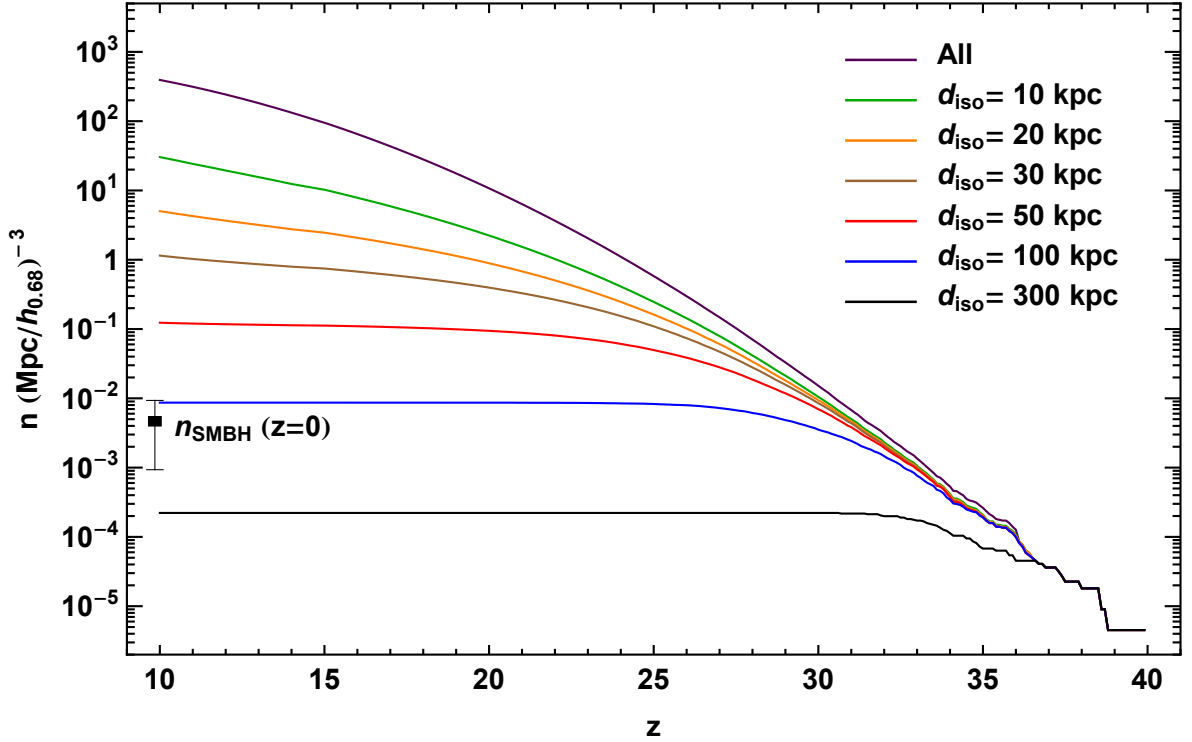


Figure 1. Evolution of comoving total number density of Pop III.1 stars and their SMBH remnants for different values of d_{iso} ranging from 10 to 300 kpc. The number density of all dark matter halos with $M > 10^6 M_{\odot}$ is also shown for reference. The data point $n_{\text{SMBH}}(z=0)$ drawn schematically on the left side of the figure shows an estimate for the present day number density of SMBHs assuming one SMBH is present in all galaxies with $L > L_{\text{min}}$. The solid square shows this estimate for $L_{\text{min}} = 0.33L_*$, while the lower and upper bounds assume $L_{\text{min}} = 0.1L_*$ and L_* , respectively.

Figure 1 shows the redshift evolution of the comoving total number density, n , of Pop III.1 stars and remnants (i.e., assumed in this model to be SMBHs) for different values of d_{iso} ranging from 10 to 300 kpc. As we will see below, for the assumption of a 10 Myr lifetime of Pop III.1 stars, these totals soon become dominated by SMBHs. Within this simulated $(60.47 h_{0.68}^{-1} \text{ Mpc})^3$ comoving volume, Pop III.1 stars start forming just after $z = 40$. For large values of d_{iso} , the number of new Pop III.1 sources decreases more quickly and n asymptotes to a constant value. For example, for $d_{\text{iso}} = 100$ kpc Pop III.1 stars have largely ceased to form by $z \sim 25$, while for $d_{\text{iso}} = 10$ kpc they continue to form still at $z = 10$.

Comparison of the number density of sources formed in these models with the present day ($z = 0$) number density of SMBHs, n_{SMBH} , constrains d_{iso} . We estimate $n_{\text{SMBH}}(z = 0) \sim 0.015 (\text{Mpc}/h)^{-3} = 0.0046 (\text{Mpc}/h_{0.68})^{-3}$ by assuming that all galaxies with $L_{\text{min}} > 0.33L_*$ host SMBHs and integrating over the local galaxy luminosity function assumed to be a Schechter function of the form

$$\phi(L) = \left(\frac{\phi^*}{L^*}\right) \left(\frac{L}{L^*}\right)^{\alpha} e^{-(L/L^*)} \quad (1)$$

where $\phi^* = 1.6 \times 10^{-2} (\text{Mpc}/h)^{-3} = 4.9 \times 10^{-3} (\text{Mpc}/h_{0.68})^{-3}$ is the normalization density and L^* is the characteristic luminosity corresponding to $M_B = -19.7 + 5 \log h = -20.55$ (e.g., Norberg et al. 2002) and α is the power law slope at low L . This value is shown on the left edge of Figure 1, with the error bar resulting from assuming $L_{\min} = 0.1$ to $1 L_*$, i.e., a range from $9.3 \times 10^{-3} (\text{Mpc}/h_{0.68})^{-3}$ to $9.3 \times 10^{-4} (\text{Mpc}/h_{0.68})^{-3}$. For comparison, integrating the SMBH mass function from Vika et al. (2009), we estimated the number density of SMBH to be $0.00879 (\text{Mpc}/h_{0.68})^{-3}$, which is consistent with our more simplistic estimate.

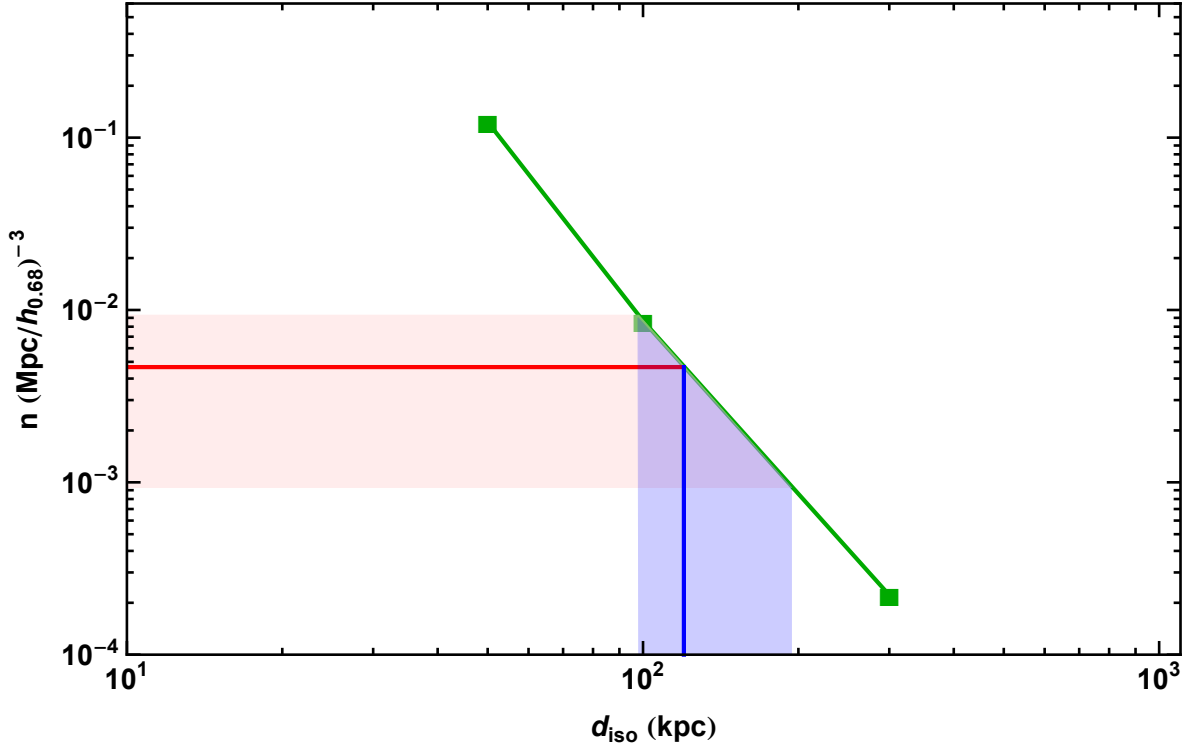


Figure 2. Asymptotic ($z = 10$) number density of SMBHs, n , versus d_{iso} . The green squares show results for the analysis with $d_{\text{iso}} = 30, 50$ and 100 kpc, joined by the green lines assuming a power law dependence of n on d_{iso} . The red line indicates $n_{\text{SMBH}}(z = 0)$ corresponding to $L_{\min} = 0.33L_*$ and the red band shows the range of n_{SMBH} corresponding to $L_{\min} = 0.1$ to $1 L_*$. The blue line and band show the corresponding value and range of d_{iso} , respectively, implied by this range of n .

Note when comparing with $n_{\text{SMBH}}(z = 0)$ that the model n does not account for any decrease due to merging of SMBHs. However, we can assess how many mergers occur in the simulation: for $d_{\text{iso}} = 50$ kpc only $\sim 0.2\%$ of SMBHs suffer a merger with another SMBH by $z = 10$, i.e., it is a very minor effect. Some additional SMBH mergers will occur at $z < 10$, but given the low rate of merging at $z > 10$ and the low fraction of $> 10^9 M_{\odot}$ halos at $z = 10$ that host SMBHs (for $d_{\text{iso}} = 50$ kpc this is $\simeq 0.16$, discussed below), it seems unlikely that this will lead to more than a factor of three reduction in n . Thus we consider that the cases of $d_{\text{iso}} = 50$ and 100 kpc are the most relevant in the context of this model of Pop III.1 seeds for forming the whole cosmic population of SMBHs. From here on we will focus on the cases between $d_{\text{iso}} = 30$ and 300 kpc.

If we assume SMBH mergers are negligible, then we can use the asymptotic (i.e., $z = 10$) number density of SMBH remnants for the cases of $d_{\text{iso}} = 50$ to 300 kpc to estimate the range of d_{iso} that is implied by our adopted constraint on $n_{\text{SMBH}}(z = 0)$. This is shown in Figure 2 as a blue shaded band, i.e., implying $100 \text{ kpc} \lesssim d_{\text{iso}} \lesssim 200 \text{ kpc}$.

Figure 3 shows the separate evolution of the comoving number density of Pop III.1 stars, SMBH remnants and the total of these two components for $d_{\text{iso}} = 30, 50, 100$ and 300 kpc. Pop III.1 stars dominate at very early times, while SMBHs dominate at later times. For $d_{\text{iso}} \gtrsim 100$ kpc the Pop III.1 star formation rate (SFR) peaks at $z \simeq 30$ and effectively stops below $z \simeq 25$, while for smaller values there can still be significant new Pop III.1 sources forming at $z = 10$. The detection or non-detection of Pop III.1 supermassive stars at $z \simeq 10$, potentially possible with JWST, could help to distinguish between these models.

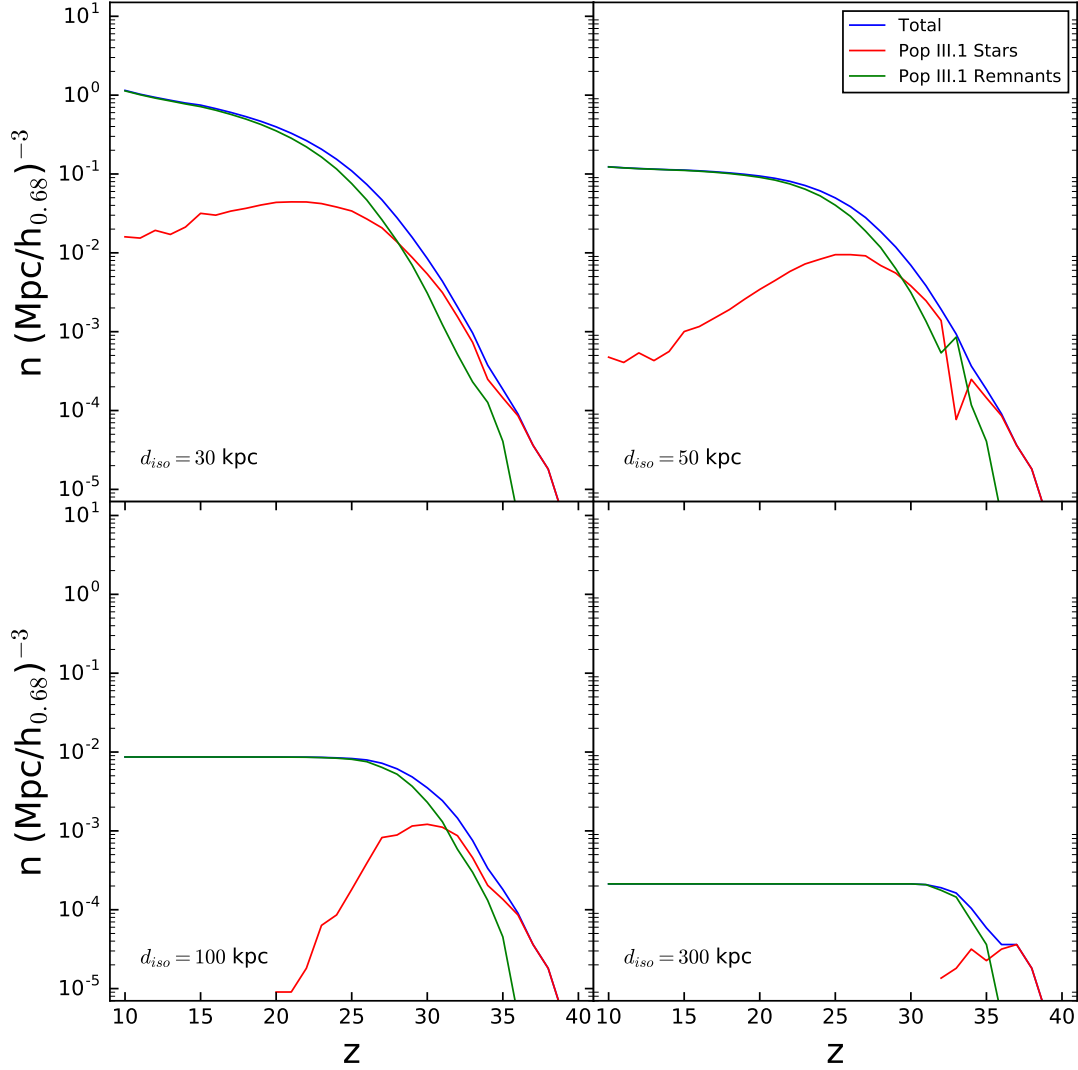


Figure 3. Evolution of the comoving number density of Pop III.1 stars, SMBH remnants and the total number of sources (shown separately) for $d_{\text{iso}} = 30$ kpc (top left), 50 kpc (top right), 100 kpc (bottom left) and 300 kpc (bottom right).

3.2. Effects of Cosmic Variance and σ_8

We study how the results are affected by cosmic variance by running several simulations of smaller volumes of $(10 h^{-1} \text{ Mpc})^3 = (14.76 h_{0.68}^{-1} \text{ Mpc})^3$ and $(20 h^{-1} \text{ Mpc})^3 = (29.52 h_{0.68}^{-1} \text{ Mpc})^3$. For each of these volumes, five independent simulations were run using different random seeds to generate the initial conditions. Figure 4 shows the results of these runs for the number density evolution of Pop III.1 stars and SMBH remnants for the case of $d_{\text{iso}} = 100$ kpc. We see that while there is moderate variation in redshift of the first Pop III.1 source in each volume, the dispersion in the final number densities of sources (i.e., for $z \lesssim 25$) in these simulations is very minor.

Halo number densities will depend on cosmological parameters; especially, the number of rare objects is mostly sensitive on the normalization of the power spectrum σ_8 . Thus next we examine how the choice of σ_8 affects the number density of Pop III.1 stars and SMBHs. We have explored a range of $\sigma_8 = 0.830 \pm 0.015$ (Planck collaboration 2015). Figure 5 shows the effect of varying σ_8 by this amount on the total number density of Pop III.1 stars and SMBHs for the case of $d_{\text{iso}} = 100$ kpc for a simulation of a $(29.52 h_{0.68}^{-1} \text{ Mpc})^3$ volume. Again the dispersion in the

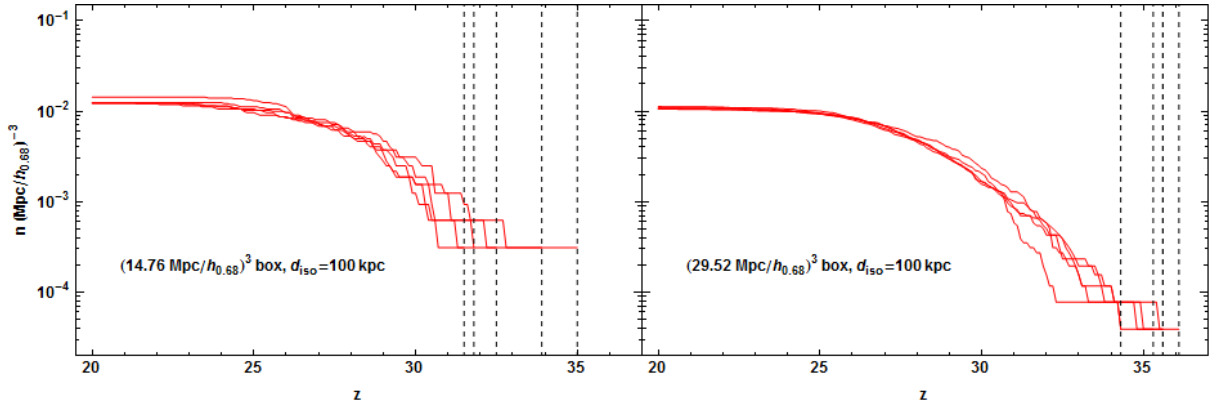


Figure 4. (a) Left: Evolution of the comoving total number density of Pop III.1 stars and their SMBH remnants for $d_{\text{iso}} = 100$ kpc. in five realizations of a $(14.76 h_{0.68}^{-1} \text{ Mpc})^3$ volume. The vertical dashed lines indicate the redshift of the appearance of the first halo in each run. (b) Right: As (a), but now showing results for five realizations of a $(29.52 h_{0.68}^{-1} \text{ Mpc})^3$ volume.

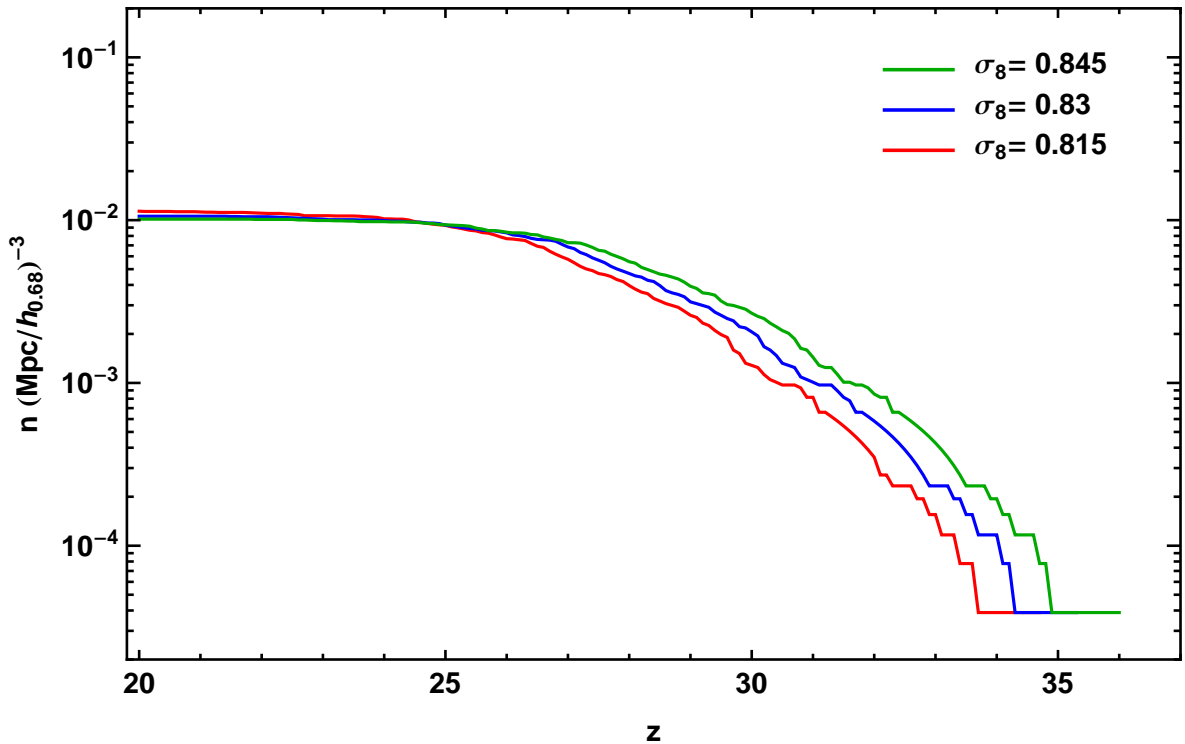


Figure 5. Effect of σ_8 uncertainties on the evolution of comoving total number density of Pop III.1 stars and their SMBH remnants for $d_{\text{iso}} = 100$ kpc. These results are based on simulations of a $(29.52 h_{0.68}^{-1} \text{ Mpc})^3$ volume.

final number densities of sources (i.e., for $z \lesssim 25$) in these simulations is very minor.

3.3. Mass Function of SMBH-Host Halos

The halos which form Pop III.1 stars and host their SMBH remnants are then followed to lower redshifts, as far as $z = 10$. These halos grow in mass by accreting dark matter particles and merging with other identified halos. In a

merger the more massive halo retains its identity. For values of $d_{\text{iso}} \gtrsim 50$ kpc, the halos that are merging with the SMBH-hosting halos are typically of lower mass and do not host SMBHs. Occasionally, they are more massive, in which case the SMBH-hosting character of the halo is transferred to this new halo identity. Even more rare is a merger of two halos that both host SMBHs. The properties of these binary SMBH halos and predictions for the eventual merger of the SMBHs will be presented in a future paper in this series. Here we focus simply on the mass function of the SMBH-hosting halos: Figure 6 shows the distribution of these masses at $z = 10$ and 15 for cases of $d_{\text{iso}} = 50$ and 100 kpc. For comparison, we also show the mass function of all halos at $z = 15$ and 10 with dotted histograms.

For $d_{\text{iso}} = 100$ kpc we see that at $z = 15$ the typical SMBH-host halo has $\sim 10^8 M_{\odot}$, while by $z = 10$ this has grown to close to $\sim 10^9 M_{\odot}$. In comparison, for $d_{\text{iso}} = 50$ kpc, SMBHs are more numerous and at a given redshift tend to occupy lower mass halos.

In general, the most massive halos, $\gtrsim 10^{10} M_{\odot}$, have the highest occupation fractions of SMBHs. By $z = 10$ this occupation fraction is close to unity for $d_{\text{iso}} = 50$ kpc and slightly smaller for $d_{\text{iso}} = 100$ kpc. However, the fraction of $> 10^9 M_{\odot}$ halos at $z = 10$ that host SMBHs is only 0.16 for $d_{\text{iso}} = 50$ kpc and 0.05 for $d_{\text{iso}} = 100$ kpc. These small fractions indicate the sparseness of SMBHs among these early galaxies for these relatively large values of d_{iso} . This suggests that in these models mergers of SMBHs will continue to be relatively rare at $z < 10$, especially for the $d_{\text{iso}} = 100$ kpc case.

3.4. Synthetic Sky Maps

Given the considerations of the local SMBH number density and the results shown in Figure 1, we again focus on the cases of $d_{\text{iso}} = 50$ and 100 kpc, with the latter being the preferred, fiducial case. For reference, at $z = 10, 15, 20, 30, 40$ the angular size of the box is $21.53', 19.84', 18.93', 17.93', 17.37'$ respectively.

To make an approximate synthetic sky map of the SMBH population (which may manifest themselves as AGN), we simply project through the entire volume of the box, adopting a constant, fixed redshift. This approximation ignores the finite light travel time across the thickness of the box, which means that the projection of the total source population is roughly equivalent to observing a finite redshift interval of the real universe. At $z = 10, 15, 20$ these redshift intervals are $\Delta z = 0.28, 0.49, 0.75$, respectively. Of course for direct comparison with AGN populations one would also need to model the duty cycle of emission and the luminosity function and spectral energy distribution properties of the accreting SMBHs. Such modeling requires making many uncertain assumptions and is beyond the scope of the present paper.

Figure 7 shows maps of the SMBH populations for $d_{\text{iso}} = 50, 100, 300$ kpc at $z = 10$. In the first case, there are still Pop III.1 stars present (assuming their lifetime is 10 Myr, see above), and these are shown in a separate map. This figure shows the dramatic effect of d_{iso} on the number of SMBH remnants predicted by the model. Their angular clustering properties will be examined below.

Figure 8 shows synthetic maps at $z = 10$ and 15, separating out different mass halos that are hosting Pop III.1 stars and SMBHs for the cases of $d_{\text{iso}} = 50$ and 100 kpc. The evolution of the typical SMBH host halo towards higher masses as the universe evolves towards lower redshift can be seen. The lower mass halos tend to be the SMBHs that have formed most recently and, at least in the $d_{\text{iso}} = 50$ kpc case where there are significant numbers, these show distinctive clustering properties compared to the more massive, typically older, sources.

3.5. Angular Correlation

We calculate the two point angular correlation function (2PACF) of $d_{\text{iso}} = 50$ and 100 kpc remnants. The angular correlation function tells us how the projection of these remnants are correlated compared to a Poisson distribution. We use a random catalog with 50 times the number of halos as in the SMBH sample, implementing the Landy-Szalay estimator to calculate the angular correlation function, $\omega(\theta)$:

$$\omega(\theta) = \frac{DD - 2DR + RR}{RR}, \quad (2)$$

where DD represents the total weight of pairs of halos from the data (i.e., the SMBHs) within each bin, RR represents the weight of pairs from the random Poisson catalog, and DR represents the weight of pairs with one particle from the data and one from the random catalog. We used the *TreeCorr* code (Jarvis et al. 2004) for these correlation calculations.

Figure 9 shows $\omega(\theta)$ for the cases of $d_{\text{iso}} = 50$ and 100 kpc observed at $z = 10$ (see Fig. 7). These have 27,122 and 1,913 SMBH sources, respectively. To increase the signal to noise we have observed the simulation volume at $z = 10$ from the three orthogonal directions and combined the results. Overall the 2PACFs of both cases are relatively flat,

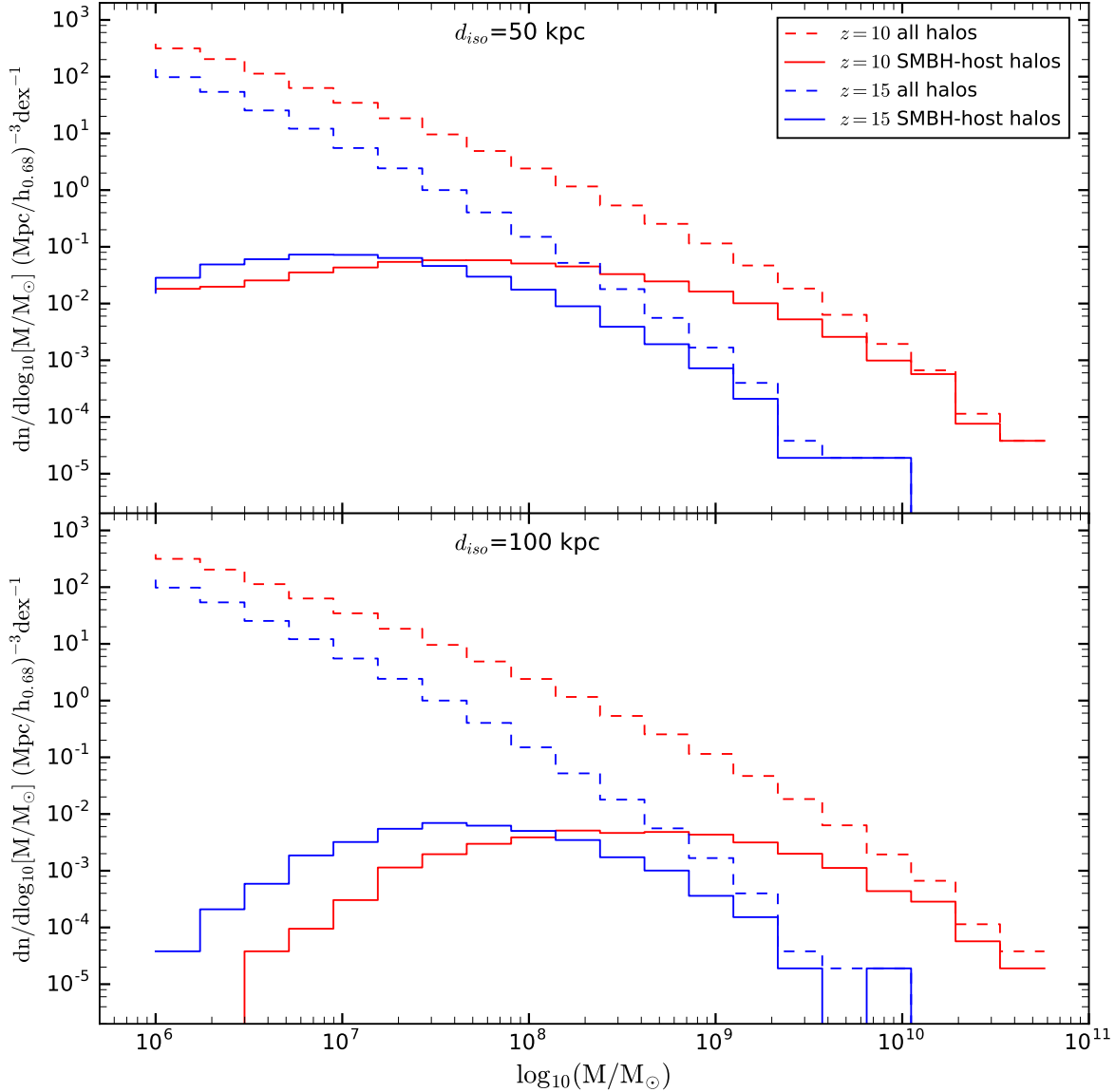


Figure 6. The mass function of SMBH-host halos at $z = 10, 15$ and for $d_{\text{iso}} = 50, 100$ kpc. These results are based on the fiducial simulation of a $(60.47 h_{0.68}^{-1} \text{ Mpc})^3$ volume.

especially compared to that of all halos with masses $> 10^9 M_{\odot}$, which is shown by the green dashed line in these figures. For $d_{\text{iso}} = 50$ kpc, there is a sign of modest excess clustering signal on angular scales $\lesssim 50''$. For $d_{\text{iso}} = 100$ kpc, with a smaller number of sources and thus larger Poisson uncertainties, there is hint of a decrease of $\omega(\theta)$ below the Poisson level on scales $\lesssim 50''$. This could be related to the angular scale of the 100 kpc proper distance of the feedback distance d_{iso} at $z \sim 30$, which corresponds to a comoving distance of ~ 3 Mpc. By $z = 10$ this corresponds to an angular scale of $64''$. Thus the signature of feedback cleared bubbles, which have a deficit of SMBHs due to destruction of Pop III.1 seeds, may be revealed in the angular correlation function. In particular, effective feedback suppression of neighboring sources leads to a relatively flat angular correlation function.

4. DISCUSSION AND CONCLUSIONS

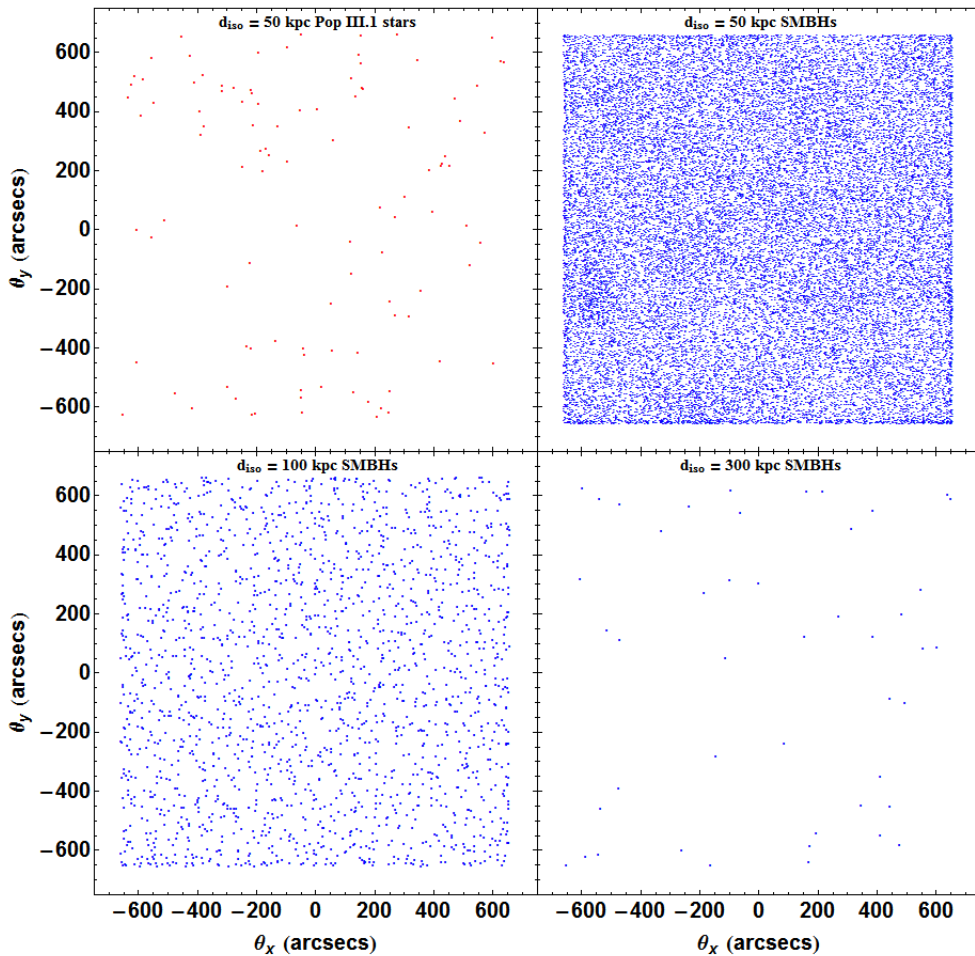


Figure 7. Synthetic maps at $z = 10$ of the $(60.47 h_{0.68}^{-1} \text{ Mpc})^3$ comoving box (projection equivalent to $\Delta z = 0.28$) of $d_{\text{iso}} = 50$ kpc Pop III.1 stars (top left) and SMBH remnants (top right). For $d_{\text{iso}} = 100$ and 300 kpc, there are no Pop III.1 stars left by $z = 10$. The SMBH remnants for these cases are shown in the lower left and lower right panels, respectively.

We have presented a model for the formation of supermassive black holes from the remnants of special Population III stars, i.e., Pop III.1 stars that form in isolation from other astrophysical sources. The physical mechanism motivating this scenario involves the Pop III.1 protostar being supported by WIMP dark matter annihilation heating (Spolyar et al. 2008; Natarajan et al. 2009), so that it retains a large photospheric radius while it is accreting. This reduces the influence of ionizing feedback on the protostar’s own accretion (McKee & Tan 2008), allowing it gather most of the $\sim 10^5 M_{\odot}$ of baryons present in the host minihalo. While many of the details of this scenario remain to be explored, our approach here has been to focus on the Pop III.1 star and SMBH populations that form in such a model, particularly their dependencies on the isolation distance, d_{iso} , that is needed for Pop III.1 formation.

Assuming that all SMBHs are produced by this mechanism, we have found that to produce the required number density of sources that can explain local ($z = 0$) SMBH populations requires $d_{\text{iso}} \sim 100$ kpc (proper distance). With such values of d_{iso} we do not expect mergers of SMBHs to be too significant. For this model the formation of Pop III.1 stars and thus SMBHs peaks at $z \simeq 30$ and is largely completed by $z = 20$. By $z = 10$ the SMBHs tend to reside in halos $\gtrsim 10^8 M_{\odot}$, extending up to $\sim 10^{11} M_{\odot}$. The angular correlation function of these sources at $z = 10$ is very flat, with little deviation from a random distribution, which we expect is a result of a competition between source feedback and the intrinsic clustering expected from hierarchical structure formation.

The preferred value of $d_{\text{iso}} \sim 100$ kpc proper distance has implications for the physics of the process. The size of the ionized zone (Strömgren radius) around a source that is ionizing the diffuse cosmological gas at $z = 30$ (we assume the baryon density is $\rho_b = 0.1574\rho_c$, where ρ_c is the critical density with $\rho_c(z = 30) = 8.01 \times 10^{-26} \text{ g cm}^{-3}$, and the

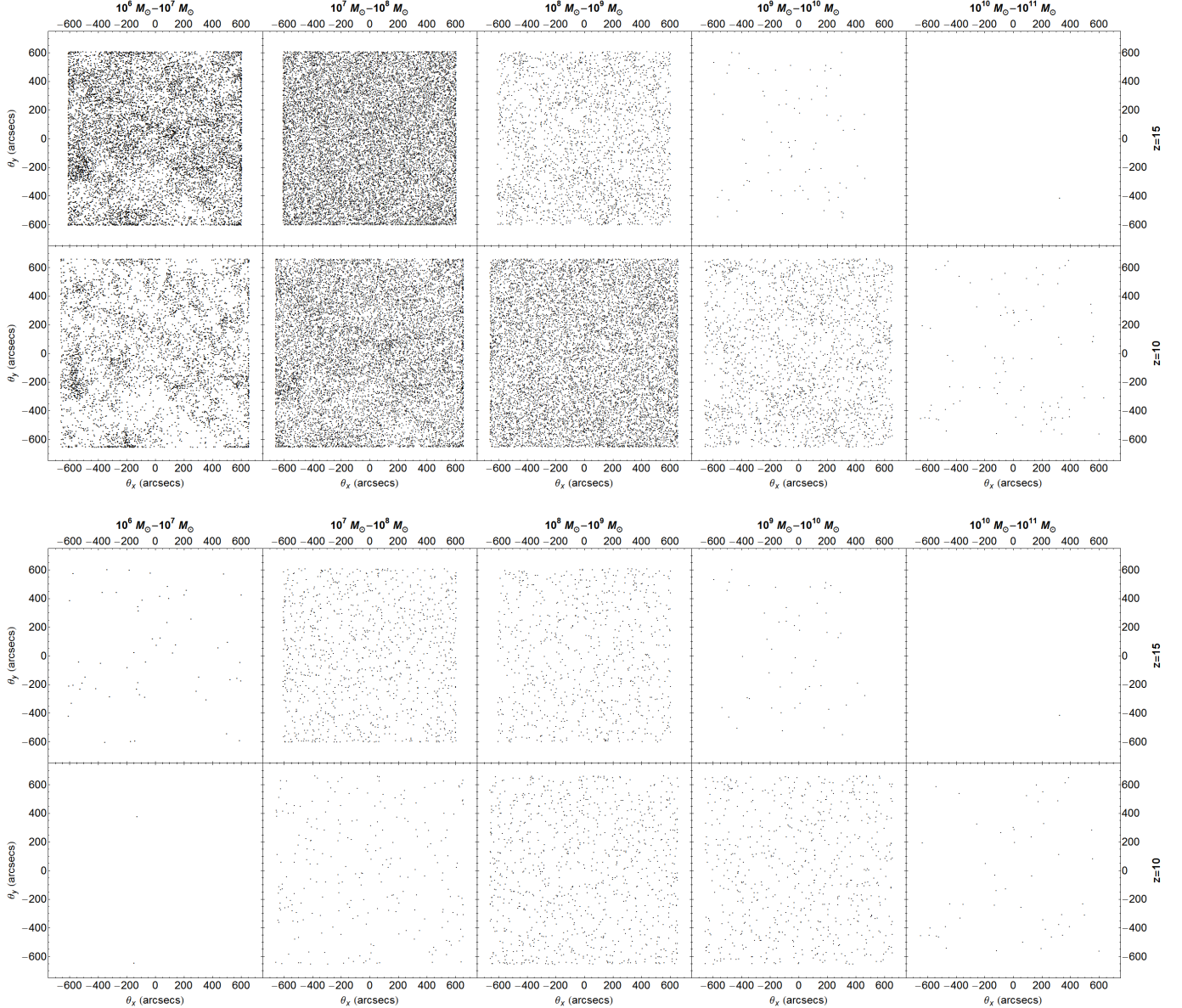


Figure 8. (a) Top panel: Synthetic maps at $z = 15$ (top row) and $z = 10$ (bottom row) of $d_{\text{iso}} = 50$ kpc Pop III.1 stars and SMBH remnants for mass bins from left column to right column of $10^6 - 10^7 M_{\odot}$, $10^7 - 10^8 M_{\odot}$, $10^8 - 10^9 M_{\odot}$, $10^9 - 10^{10} M_{\odot}$ and $10^{10} - 10^{11} M_{\odot}$. (b) Bottom panel: As (a), but now for $d_{\text{iso}} = 100$ kpc.

mass per H is $\mu_{\text{H}} = 2.20 \times 10^{-24}$ g, given $n_{\text{He}} = 0.08n_{\text{H}}$) is

$$r_{\text{HII}} = 59.6 S_{53}^{1/3} T_{3e4}^{0.27} (n_{\text{H}}/n_{\text{H},z=30})^{2/3} \text{ kpc}, \quad (3)$$

where we have normalized to an ionizing photon luminosity of $S_{53} = S/10^{53} \text{ s}^{-1} = 1$, which is an approximate estimate for that expected for a $10^5 M_{\odot}$ Pop III zero age main sequence star (e.g., extrapolating linearly ($S \propto m_*$ from the models shown in Tan & McKee 2004, which extend up to $m_* = 10^3 M_{\odot}$) that may appear as part of the evolution from Pop III.1 protostar to SMBH remnant. We have also normalized to an ionized gas temperature of $T_{3e4} = T/30,000 \text{ K} = 1$, appropriate for primordial composition gas and assumed singly ionized He.

It is striking that this simple estimate for a feedback radius due to ionizing feedback is very similar to the values of d_{iso} that are required by this scenario of Pop III.1 seeds of SMBHs to explain the local number density of these sources. Of course, much more detailed exploration of the feedback from supermassive Pop III.1 stars is needed in the context of this scenario, which will be the subject of a future paper in this series.

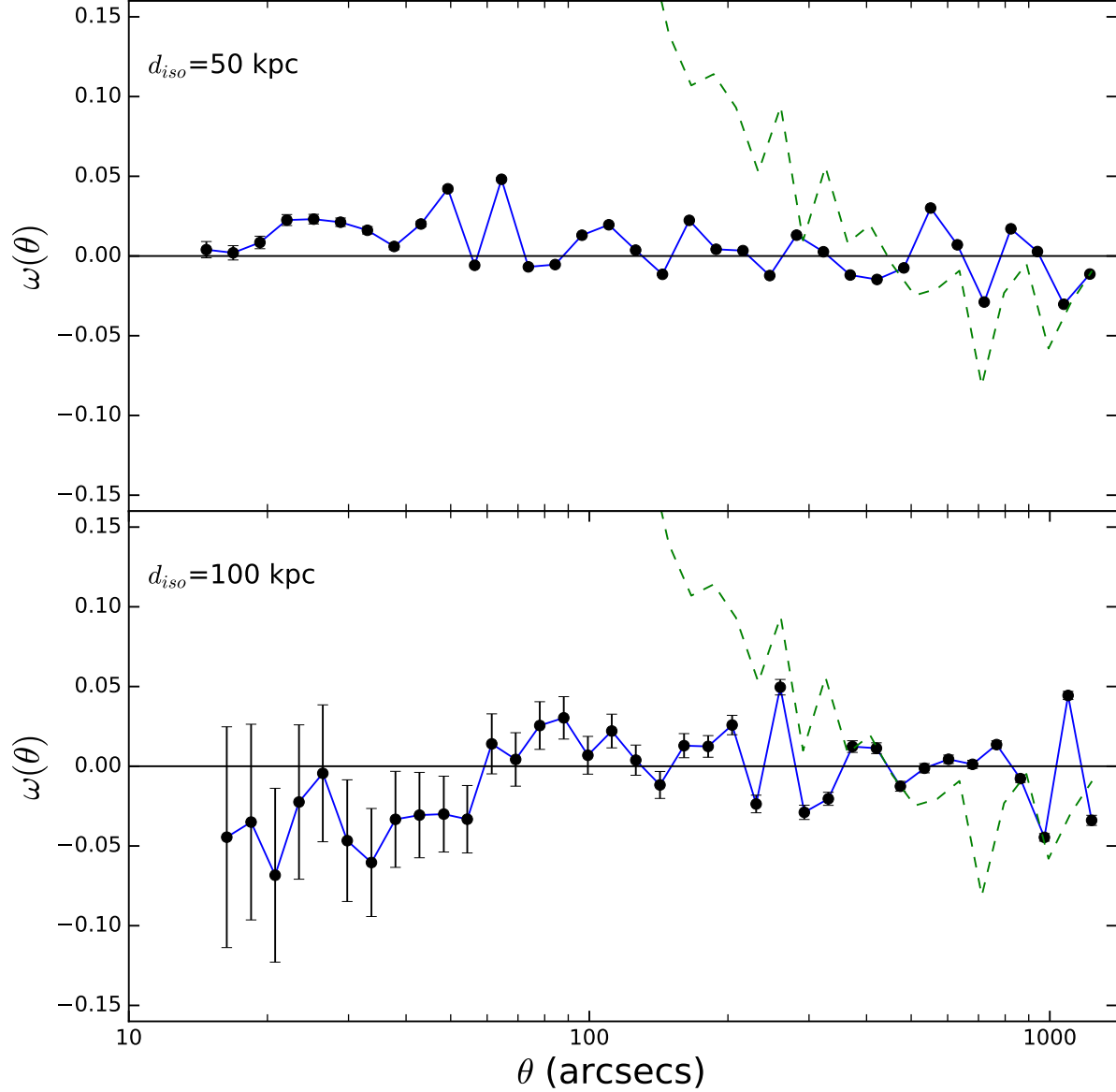


Figure 9. 2PACF of $d_{iso} = 50$ and $d_{iso} = 100$ kpc remnants at $z = 10$. The error bars indicate shot noise in each angular separation bin. For comparison we have also plotted the 2PACF of all the halos with mass greater than $10^9 M_{\odot}$ at $z = 10$ (green dashed curve). It rises sharply at small scales, which shows they are highly clustered (it reaches a value of ~ 0.22 at $10''$ and ~ 0.57 at $20''$).

We thank Peter Behroozi, Krittapas Chanchaiworawit, Mark Dijkstra, Alister Graham, Lucio Mayer, Rowan Smith, Kei Tanaka, Brian Yanny and an anonymous referee for helpful comments and discussions. Fermilab is operated by Fermi Research Alliance, LLC, under Contract No. DE-AC02-07CH11359 with the U.S. Department of Energy. NB is supported by the Fermilab Graduate Student Research Program in Theoretical Physics. JCT acknowledges NSF grant AST 1212089.

REFERENCES

Abel, T, Bryan, G. L., & Norman M. L. 2002, *Science*, 295, 93

Ackermann, M. et al. (Fermi-LAT Collaboration) 2015, *Phys. Rev. Lett.* 115, 221301

- Agnese, R. et al. (SuperCDMS Collaboration) 2014, *Phys. Rev. Lett.* 112, 241302
- Aguirre, J. E., Ginsburg, A. G., Dunham, M. K., et al. 2011, *ApJS*, 192, 4
- Begelman, M. C., Volonteri, M., & Rees, M. J. 2006, *MNRAS*, 370, 289
- den Brok, M., Seth, A. C., Barth, A. J. et al. 2015, *ApJ*, 809, 101
- Bromm, V., Coppi, P. S. & Larson, R. B. 2002, *ApJ*, 564, 23
- Bromm, V. & Loeb, A. 2003, *ApJ*, 596, 34
- Buchert, T. & Ehlers, J. 1993, *MNRAS*, 264, 375
- Catelan, P. 1995, *MNRAS*, 276, 115
- Clark, P. C., Glover, S. C. O., Smith, R. J., Greif, T. H., Klessen, R. S., & Bromm, V. 2011, *Science*, 331, 1040
- Devecchi, B., Volonteri, M., Rossi, E. M., Colpi, M., & Portegies Zwart, S. 2012, *MNRAS*, 421, 1465
- Dijkstra, M., Haiman, Z., & Spaans, M. 2006, *ApJ*, 649, 14
- Dijkstra, M., Ferrara, A., & Mesinger, A. 2014, *MNRAS*, 442, 2036
- Ferrara, A. & Loeb, A. 2013, *MNRAS*, 431, 2826
- Freitag, M., Gürkan, M. A., & Rasio, F. A. 2006, *MNRAS*, 368, 141
- Graham, A. W. 2016, *ASSL*, 418, 263
- Graham, A. W., Onken, C. A., Athanassoula, E., & Combes, F. 2016, *MNRAS*, 412, 2211
- Greif, T. H. & Bromm, V. 2006, *MNRAS*, 373, 128
- Greif, T. H., Springel, V., White, S. D. M., Glover, S. C. O., Clark, P. C., Smith, R. J., Klessen, R. S. & Bromm, V. 2011, *ApJ*, 737, 75
- ürkan, M. A., Freitag, M., & Rasio, F. A. 2004, *ApJ*, 604, 632
- Haehnelt, M. G. & Rees, M. J. 1993, *MNRAS*, 263, 168
- Hennebelle, P., Commerçon, B., Joos, M. et al. 2011, *A&A*, 528, 72
- Hirano, S., Hosokawa, T., Yoshida, N. et al. 2014, *ApJ*, 781, 60
- Hosokawa, T., Omukai, K., Yoshida, N. & Yorke, H. W. 2011, *Science*, 334, 1250
- Inayoshi, K. & Omukai, K. 2012, *MNRAS*, 422, 2539
- Inayoshi, K., Visbal, E., & Kashiyama, K. 2015, *MNRAS*, 453, 1692
- Jarvis, M., Bernstein, G., & Jain, B. 2004, *MNRAS*, 352, 338
- Johnson, J. L., & Bromm, V., 2007, *MNRAS*, 374, 1557
- Khachatryan, V. et al. (CMS Collaboration) 2016, *Phys. Rev. D*, 93, 052011
- Kormendy, J. & Ho, L. C. 2013, *ARA&A*, 51, 511
- Latif, M. A. & Schleicher, D. R. G. 2016, *A&A*, 585, 151
- Mayer, L., Kazantzidis, S., Escala, A., & Callegari, S. 2010, *Nature*, 466, 1082
- Mayer, L., Fiacconi, D., Bonoli, S., Quinn, T., Roskar, R., Shen, S. & Wadsley, J. 2015, *ApJ*, 810, 51
- McKee, C. F. & Tan, J. C. 2008, *ApJ*, 681, 771
- Milosavljević, M., Bromm, V., Couch, S. M., & Oh, S. P. 2009, *ApJ*, 698, 766
- Monaco, P., Theuns, T., & Taffoni, G. 2002, *MNRAS*, 331, 587
- Monaco, P., Sefusatti, E., Borgani, S. et al. 2013, *MNRAS*, 433, 2389
- Mortlock, D. J., Warren, S. J., Venemans, B. P. et al. 2011, *Nature*, 474, 616
- Moutarde, F., Alimi, J.-M., Bouchet, F. R. et al. 1991, *ApJ*, 382, 377
- Munari, E., Monaco, P., Sefusatti, E. et al. 2016, *arXiv:1605.04788*
- Natarajan, A., Tan, J. C. & O’Shea, B. W. 2009, *ApJ*, 692, 574
- Norberg, P., Cole, S., Baugh, C. et al. 2002, *MNRAS*, 336, 907
- O’Shea, B. W., Abel, T., Whalen, D. & Norman, M. L. 2005, *ApJ Lett.*, 628, L5
- O’Shea, B. W. & Norman, M. L. 2006, *ApJ*, 654, 66
- Planck Collaboration: Ade, P. A. R., Aghanim, N., Arnaud, M. et al. 2015, *arXiv:1502.01589*
- Portegies Zwart, S. F., Baumgardt, H., Hut, P., Makino, J., & McMillan, S. L. W. 2004, *Nature*, 428, 724
- Price, D. J. & Bate, M. R. 2007, *MNRAS*, 377, 77
- Schleicher, D. R. G., Banerjee, R., Sur, S. et al. 2010, *A&A*, 522, 115
- Schober, J., Schleicher, D. R. G., Federrath, C. et al. 2012, *ApJ*, 754, 99
- Shankar, F., Bernardi, M., Sheth R. K. et al. 2016, *MNRAS*, 460, 3119
- Smith, R. J., Iocco, F., Glover, S. et al. 2012, *ApJ*, 761, 154
- Spolyar, D., Bodenheimer, P., Freese, K., & Gondolo, P. 2009, *ApJ*, 705, 1031
- Spolyar, D., Freese, K., & Gondolo, P. 2008, *Phys. Rev. Lett.*, 100, 051101
- Stacy, A., Pawlik, A. H., Bromm, V. & Loeb, A. 2014, *MNRAS*, 441, 822
- Susa, H., Hasegawa, K. & Tominaga, N. 2014, *ApJ*, 792, 32
- Tan, J. C. & Blackman, E. G. 2004, *ApJ*, 603, 401
- Tan, J. C. & McKee, C. F. 2004, *ApJ*, 603, 383
- Tan, J. C., Smith B. D., & O’Shea, B. W. 2010, *AIPC*, 1294, 34
- Turk, M. J., Abel, T. & O’Shea, B. W. 2009, *Science*, 325, 601
- ink, J. S. 2008, *New Astron. Rev.*, 52, 419
- Vika, M., Driver, S. P., Graham, A. W. and Liske, J. 2009, *MNRAS*, 400, 1451.
- Whalen, D. & Norman, M. L. 2006, *ApJS*, 162, 281
- Whalen, D., O’Shea, B. W., Smidt, J., & Norman, M. L. 2008, *ApJ*, 679, 925